$$f_{ck,c} = f_{ck} + 3.7 f_{c2} \tag{1}$$

In the event of an earthquake, the column repeatedly receives moments in different directions based on the neutral axis. This moment acts as a tensile stress and compressive stress on the column, causing nonlinear behavior of the column and failure of the concrete cover. If the rebar is buckled after removal of the cover, the core concrete loses its confinement effect, and the hoop fails. Failure behavior is shown in Fig. 1.

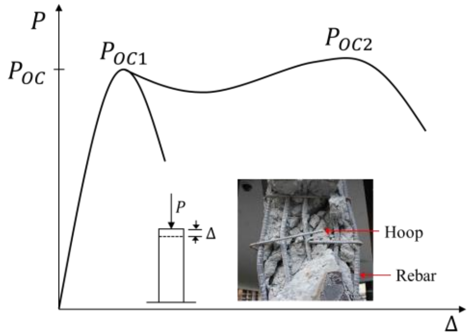

Fig. 1 Axial compressive force-displacement curve of an RC column (Kim 2019)

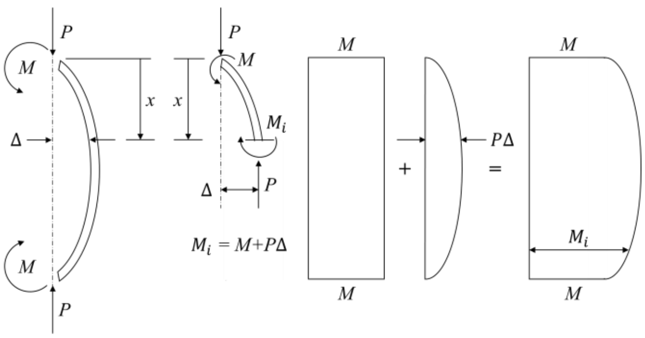

Fig. 2 Primary, secondary, and total moments of a column (Min 2013)

In columns with seismic retrofit, secondary moments occur due to geometric deformation, as shown in Fig. 2, caused by the mass and horizontal seismic force of the upper structure. Thus, these forces are applied by the buckling rebar in the web of cross-section buried in the column. Therefore, a four-point bending analysis was designed to simulate the behavior of the buckling of the rebar and apply it to seismic retrofit to determine the bending rigidity.

### *2.2 Determination of cross-section of seismic retrofit*

In this paper, a bolt fastened type was developed as a new type of seismic retrofit favorable to constructability and maintenance. The cross-section of the retrofit is T-type and is installed after removing a part of the cover of the RC column based on the thickness of the web. This reinforcement method maximizes the unification of behavior by increasing the adhesion with the column through the internal web. In addition, it is possible to strategically reinforce local plastic areas rather than reinforcement of the entire cross section, enabling easier construction. When seismic reinforcement is fastened to a RC column, stress is expected to be concentrated on the web embedded in the column more than on the flange surrounding the column. Therefore, the width and thickness of the web were set as variables for analysis.

Seismic retrofit in the form of a T-type cross-sectional bolt fastener consists of web, flange, fastener, and stiffener. The web is embedded in a column to increase constructability and flexural rigidity. The flange acts as a metal jacket surrounding the column and is connected to the fastener. During the construction process, the fastener is combined with bolts to enclose columns, with the width of the flange increasing as the number of bolts increases. Therefore, expanding the cross-section of a seismic retrofit can hinder the aesthetic, increase the manufacturing cost, and cause over-reinforcement. However, it is difficult to secure stability of a seismic retrofit because addition of only one bolt can cause torsion. Considering these characteristics, only two bolts were used.

The common thickness of the steel plate comprising the seismic retrofit is 10 mm. Considering the sizes of bolts and installation equipment used for fastening, the minimum width of the flange was set to 90 mm, and the minimum height of the fastening part was set to 50 mm. The shape of the stiffener was set to 40 mm considering the welding of the flange and fastening part. The control model sets the web thickness to 10 mm when a seismic retrofit is installed on the column. In addition, to determine the relationship between the thickness of the web and the performance of the seismic retrofit, a model with a 15-mm web was analyzed. Detailed schematics are illustrated in Figs. 3 and 4.

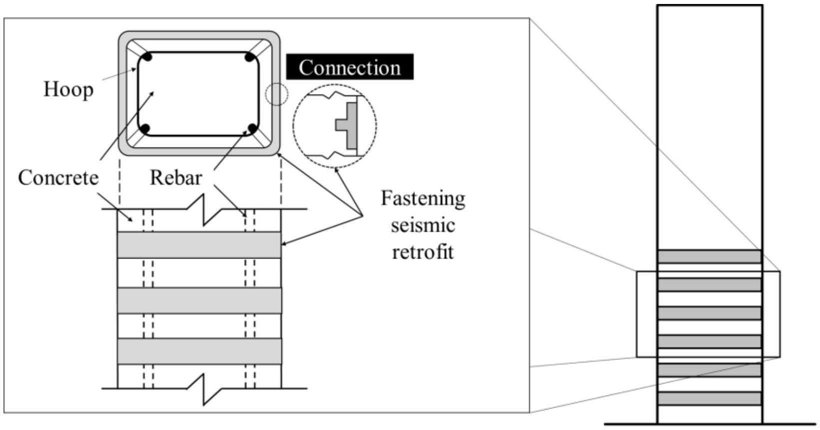

Fig. 3 Installation method of a T-type cross-section fastening retrofit

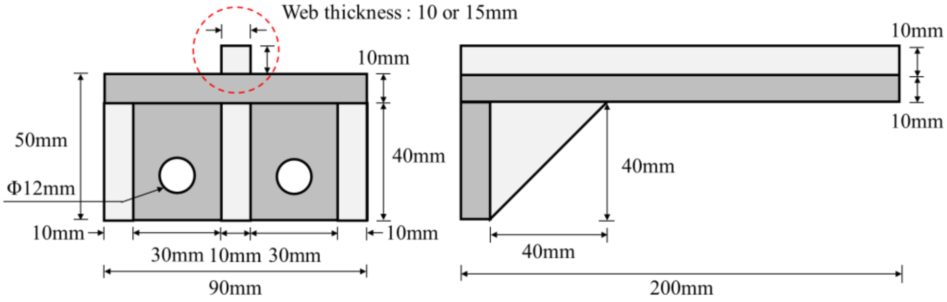

Fig. 4 Sectional and front views of a seismic retrofit

## 3. NON-LINEAR FINITE ELEMENT ANALYSIS

### *3.1 Materials*

Seismic retrofit is a type of T-type cross-sectional steel fastened by two high-tension bolts. The steel used is stainless steel SUS304, and the high-tension bolt is SCM435. The detailed properties are shown in Table 1.

Table 1 Material properties

| | Chemical composition (mass%) | | | | |
|---|---|---|---|---|---|
| | C | Cr | Ni | Si | Mn |
| SUS304 | ≤0.08 | 18.0~20.0 | 8.0~10.5 | - | - |
| SCM435 | 0.33~0.38 | 0.9~1.2 | ≤0.25 | 0.15~0.35 | 0.6~0.9 |

| | Mechanical property | | |
|---|---|---|---|
| | Yield strength (MPa) | Tensile strength (MPa) | Elongation (%) |
| SUS304 | ≥215 | ≥505 | ≥40 |
| SCM435 | 800 | 1200 | ≥14 |

SUS304 is an alloy steel of nickel and chromium that is resistant to corrosion and erosion. It has excellent heat resistance, low-temperature strength, and mechanical properties. In addition, it has a high tensile strength that exceeds that of a typical rebar and has a low yield ratio and low yield strength, which are advantageous for machining.

The high-tension bolts used for fastening are hexagonal bolts of F10T for friction bonding. This bolt follows KS B 1010 (2019) and has 900 MPa of yield strength, 1,200 MPa of ultimate tensile strength and no less than 14% elongation.

Density, Young's modulus, and Poisson ratio were established to determine material behaviors of bodies and bolts through finite element analysis. Among the materials used, the density and Poisson ratio of SUS304 used values of general steel. For this steel, the specimen in the form of a dog-bone was produced to obtain the properties of the elastic and plastic areas to be used for analysis. The stress-strain relationship was shown through tensile tests. Young’s modulus was obtained by performing a press test on the tensile test specimen. Experimental pictures are shown in Figs. 5 and 6.

Fig. 5 Tensile test of SUS304

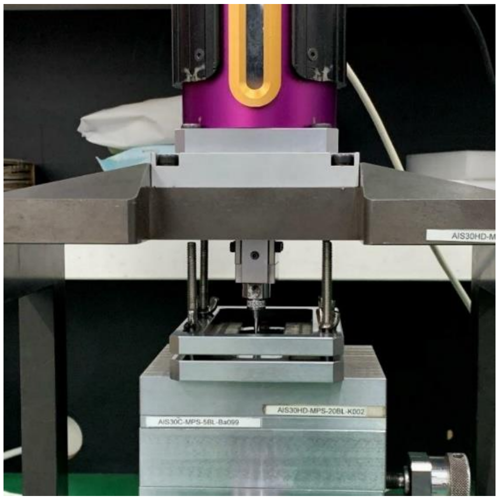

Fig. 6 Press test of SUS304

SCM435 is a material commonly used for high-tension bolts and commercial off-the-shelf products. It has universal density, Young's modulus, and Poisson ratio. The properties of each material used in the test are shown in Table 2.

Table 2 Material properties for ABAQUS

| Part | Material | Density | Young's modulus (MPa) | Poisson ratio |
|---|---|---|---|---|
| Body | SUS304 | 7.85E-09 | 162,800 | 0.3 |
| Bolt | SCM435 | 7.80E-09 | 205,000 | 0.3 |

In general, overall deformation in the bending test is accompanied by elastic and plastic behaviors of the specimen. The entire stress-strain curve must be included in finite element analysis, allowing analytical behavior in the plastic area after the elastic area to be simulated similarly to the actual environment and more accurate analysis results. To increase the accuracy of analysis, we set the plastic option, which is commonly used for steel analysis. The plastic option requires yield stress and plastic strain values, which can be derived from the stress-strain graph of the material. For SUS304, the stress-strain relationship was determined through tensile test and for SCM435, the stress-strain relationship was investigated from Noda (2016). The stress-strain curve is shown in Fig. 7.

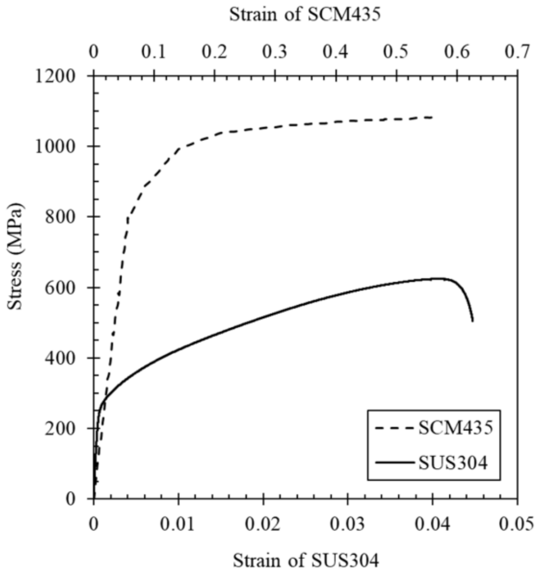

Fig. 7 Stress-strain curves of SUS304 and SCM435(Noda 2016)

In the stress-strain relationship, the values of only the plastic area were extracted and entered into the options for establishment of the governing equation after the yield point. The relationship between yield stress and plastic strain of each material is shown in Table 3.

Table 3. Yield stress-plastic strain curves of SUS304 and SCM435

| Yield stress (MPa) | | Plastic strain | |
|---|---|---|---|
| SUS304 | SCM435 | SUS304 | SCM435 |
| 240.6179 | 844.269 | 0 | 0 |
| 300.1945 | 882.213 | 0.015094775 | 0.000704 |
| 400.0033 | 991.304 | 0.069143234 | 0.0048507 |
| 500.0500 | 1041.11 | 0.134446232 | 0.0095554 |
| 600.0251 | 1057.71 | 0.201001434 | 0.0176967 |
| 700.0995 | 1069.57 | 0.263251625 | 0.0238027 |
| 800.0223 | 1076.68 | 0.322951672 | 0.0292066 |
| 900.0079 | 1086.17 | 0.384609869 | 0.0349615 |
| 986.1872 | 1100 | 0.452615865 | 0.04 |

### *3.2 Model Establishment*

A T-shaped cross-sectional fastening seismic retrofit showed symmetry as a symmetrical model. Figure 8 shows full scale and half scale models. As shown in Fig. 8, the meshes and load and boundary conditions of the fastened type seismic retrofit FEM are set up. For this, 8-node solid elements (C3D8) are applied for fastening, and the jig for support and loading is a rigid body element (R3D4). The average size of the element is 3 mm. The total number of elements is 12,135 for modeling with a 10mm web thickness and 13,344 for modeling with a 15mm web thickness.

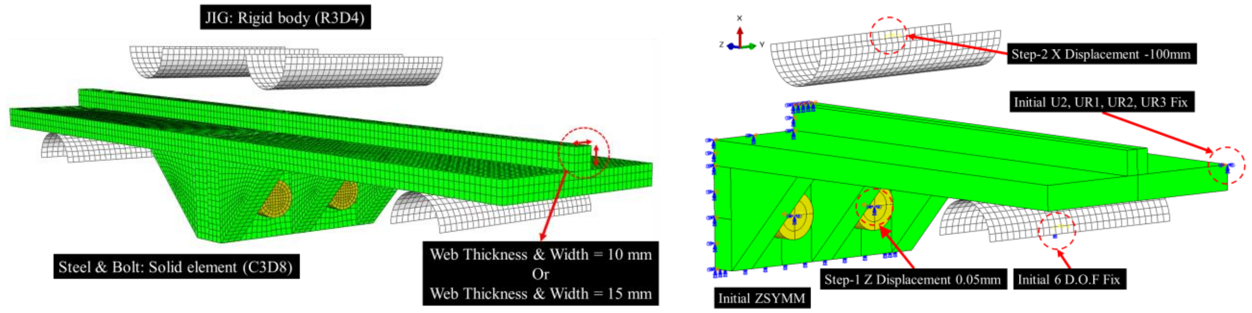

Fig. 8 Full scale and half scare models of a fastening type of seismic retrofit

Web, flange, and stiffener will be welded together and are set as Tie models for general contact in modeling. To input the axial force of the bolt, the reference point (RP) is set at the center of the bolt's head to combine the bolt and coupling.

To reduce the number of elements of the analytical model, we set it to half scale model to set the symmetry constraint ZSYMM. The lower jig constrained displacement and rotation in all directions for support. In addition, the Y-direction displacement of the free end of the model and rotation in all directions are constrained to enhance the Static General convergence. 0.05mm in the Z direction for axial force of the bolt and 100mm in the X direction displacement control for bending analysis are set in different steps.

### *3.3 Analytical results*

Curve trends in 10 mm model and 15 mm model are similar. Models with a web thickness of 10 mm had an ultimate strength of 32.59 kN, while models with an ultimate strength of 15 mm had an extreme load of 51.67 kN, which was 63% higher. This figure is significant because the ultimate strength increased by 63 % as the thickness of the web increased by 50%. The load-displacement curves are shown in Fig. 9.

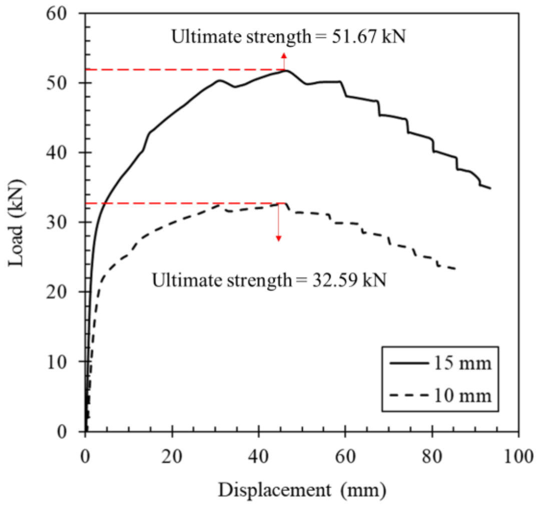

Fig. 9 Load-displacement curves of 10 mm and 15 mm models

In Fig. 10, we visually represent the results of nonlinear finite element analysis to observe variations according to web thickness size. Both 10 mm and 15 mm models show no severe deformation in the bolts, and the analysis shows a tendency for stress to be concentrated on bolts and forced area. The maximum stress for modeling with a web of 15 mm is 787.2 MPa, and the maximum stress for modeling with a web of 10 mm is 688.3 MPa. As the web thickness increased, the ultimate strength increased by 158%, while the maximum stress increased by only 114%. Therefore, increasing the size of the web is effective in increasing the performance of seismic retrofit and has a significant impact.

Also, no noticeable deformation occurred in the shape of the bolt. There is a tendency for stress to be concentrated in the screw section rather than in the head of the bolt, which is larger in models with a web of 15mm. Model with a web of 10 mm had a maximum stress of 256.1 MPa for bolts, while model with a web of 15 mm has a stress of 579.8 MPa, which is 2.3 times greater. As the size of the web has decreased, it is believed that the load that bolt has to burden has increased.

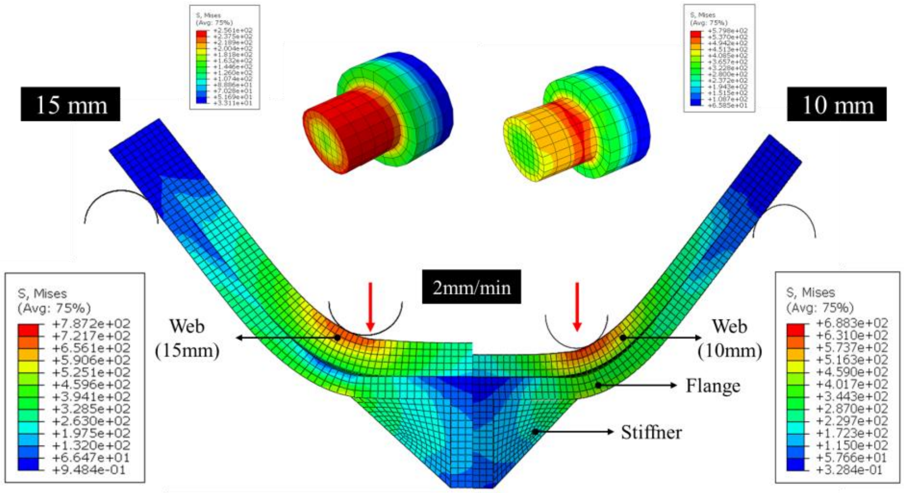

Fig. 10 Visualization of Von Mises stress of 10- and 15-mm models

## 4. CONCLUSIONS

In this paper, we developed the shape of a new type of seismic retrofit, T-type cross-section fastening retrofit. Four-point bending analysis was performed on this seismic retrofit to simulate geometric deformation caused by the mass and horizontal seismic force of the upper structure of the column, and its performance was determined. As a result of the analysis, the patterns and influence of load-displacement curves according to the thickness of the web were compared. When the web's thickness increased by 150%, the ultimate strength increased by 158% and the maximum stress increased by 114%. Therefore, it was effective to increase the performance of seismic retrofit by selecting the maximum dimensions considering concrete cover. Furthermore, no change in the shape of the bolts was observed regardless of the thickness of the web, demonstrating sufficient rigidity to engage the fastening seismic retrofit. Based on this research, it is expected that actual prototypes can be produced and contribute to the production of real product. A quasi-static experiment will be required to produce a real prototype in future studies and to simulate seismic loads by fastening to a column. In addition, it is deemed necessary to improve the applicability and practicality of fastening type seismic retrofit to the actual working environment and to further improve the seismic performance of RC columns.

### *Acknowledgement*

This work was supported by the National Research Foundation of Korea (NRF) grant funded by the Korea government (MSIT). (No. NRF-2019R1A2C1011264)

## REFERENCES

Afifi, M.Z. et al (2015), "Confinement Model for Concrete Columns Internally Confined with Carbon FRP Spirals and Hoops", *Journal of Structural Engineering*, Vol. **141**(9), 04014219.

Byun, H.S. (2020), "*Study on displacement·ductility and load bearing capacity enhancement effect of square column with continuous transverse reinforcements*", Unpublished master's thesis, Yonsei University, Seoul.

Chae, K.S. (2018), "*Study on method of continuous transverse stirrup for ductility of rectangular cross-section RC column*", Unpublished master's thesis, Yonsei University, Seoul.

Kim, J.B. (1999), "*An experimental study on strengthening effect of reinforced concrete columns strengthened with steel plates*", Unpublished doctoral dissertation, Kon-Kuk University, Seoul.

Kim, J.C., Shin, S.H. and Oh, S.H. (2019), "Damage Investigation of Pilotis Structures and Analysis of Damage Causes by Pohang Earthquake", *JAIK_SC*, Vol. **35**(3), 3-10.

KSA (2009), Set of high strength hexagon bolt, hexagon nut and plain washers for friction grip joints (KS B 1010:2009), Korea Standard Association, Seoul.

Mander, J. B., Priestley, M. J. and Park, R. (1988), "Theoretical stress-strain model for confined concrete", *Journal of structural engineering*, Vol. **114**(8), 1804-1826.

Min, C.S. (2013), *Reinforced concrete design*, Goomibook, Seoul.

MOLIT (2021), Korea Design Standard (KDS 14 20 20:2021), Ministry of Land, Infrastructure and Transport, Sejong.

Noda, N. A. et al. (2016). "Effect of pitch difference between the bolt–nut connections upon the anti-loosening performance and fatigue life". *Materials & Design*, Vol. **96**, 476-489.

Sheikh, S. A. and Yeh, C. C. (1992), "Analytical moment-curvature relations for tied concrete columns", *Journal of Structural Engineering*, Vol. **118**(2), 529-544.